Multiple Mobile Equipment Localization in Indoor Environment Based on Cell Sectoring

Viet Thuy Vu[1(✉)], Yevhen Ivanenko[1], Aman Batra[2], Mats I. Pettersson[1], and Thomas Kaiser[2]

[1] Blekinge Institute of Technology, Karlskrona, Sweden
{viet.thuy.vu,yevhen.ivanenko,mats.pettersson}@bth.se
[2] University of Duisburg-Essen, Duisburg, Germany
{aman.batra,thomas.kaiser}@uni-due.de

Abstract. Precise mobile equipment localization in indoor environment is possible for mobile equipment with an integrated radar system. Deploying an omni-directional antenna at a base station allows localizing a single mobile unit at a time slot and a frequency resource block. With cell sectoring, an approach to cope with increasing capacity in a cell of a mobile network, helps to localize multiple mobile units at a time slot and a frequency resource block. Most importantly, cell sectoring helps to avoid localization ambiguity caused by the backprojection process. The paper presents the precise multiple mobile equipment localization approach in indoor environment based on cell sectoring. The simulation illustrates the benefit of the approach. The practicality of the approach is also addressed in the paper.

Keywords: Localization · 6G · FMCW radar

1 Introduction

Several frequency ranges including D-band (110 to 175 GHz) and THz range (0.3 to 10 THz) are under consideration for 6G. Although these frequency ranges have been researched for long time they have mainly designated for astronomy and military, e.g., radar systems. Sharing the same radio frequency (RF) resources by mobile communication and radar opens the opportunity to integrate radar system on mobile equipment. Such system can be called a joint radar?communication (JRC) system [1,2]. Another name used for such systems

The authors would like to thank 2π-Labs GmbH, Germany, for providing the radar system for the research.
The research work presented in this paper was supported by the Crafoord Foundation, Sweden, ("Crafoordska stiftelsen") under Project 20230898 and by the German Research Foundation ("Deutsche Forschungsgemeinschaft") (DFG) under Project-ID 287022738 TRR 196 for Project S05.

N.-S. Vo and H.-A. Tran (Eds.): INISCOM 2023, LNICST 531, pp. 119–131, 2023.
https://doi.org/10.1007/978-3-031-47359-3_9

is a joint communication and sensing (JCAS) system. A large number of research on JRC systems has been done, focusing on the challenges of JRC front-end for 6G applications [3], waveform designa for JRC systems [4] and other technical problems [5–8].

The use cases of the next generation of mobile communication (6G) have been introduced recently by NGMN Alliance [9]. Localization at centimeter or better level, particularly in indoor environment, is listed in the class Enabling Services of the high-level grouping of use cases. A JRC system has shown the capability of precise localization in indoor environment [10–12]. In [13], different configuration to realize synthetic aperture radar (SAR) for localization on mobile equipment with integrated radar system are proposed. The movement of mobile users helps to synthesize an aperture that is much larger than the physical aperture of a radar system. In [14], a discussion about mobile user localization is presented. It is shown that a mobile unit can feasibly be localized by implementing backprojection at a base station. However, the localization ambiguity occurs as an inherit problem of a backprojection process. This can be avoided if we know the orientation of an antenna.

Cell sectoring is an approach to cope with increasing capacity in a cell of a mobile network [15]. A cell is divided into several sectors, typically three sectors, and each is with their own set of frequency resources. In common situation, omni-directional antennas are deployed at base stations. To implement cell sectoring, an omni-directional antenna is replaced by a number of directional antennas, and each is oriented to a specified sector. This approach also helps to decrease the number of interfering co-channel cells and co-channel interference, leading to the small separation between co-channel cells.

Deploying several passive receivers at a base station and orienting the directional antenna of each receiver to a specified sector allow localizing multiple mobile units in a time slot and a frequency resource block. With this arrangement, the radar measurements are in the side-looking mode. The localization ambiguity, which is caused by the backprojection process, is therefore eliminated. This approach will be presented in this paper and the approach is called the precise multiple mobile equipment localization approach in indoor environment based on cell sectoring.

The rest of the paper is organized as follows: Sect. 2 gives a summary of the precise mobile equipment localization approach in indoor environment. The multiple mobile equipment localization version based on cell sectoring is proposed in Sect. 3. Sections 4 and 5 present the simulation results and the experimental results, respectively. Section 6 provides the conclusions.

2 Precise Mobile Equipment Localization Approach in Indoor Environment

Consider a scenario given in Fig. 1. A microcell (femto or pico) is served by a base station. There are several mobile users operating in the cell. The mobile equipment is integrated with radar systems. The mobile equipment has a clear

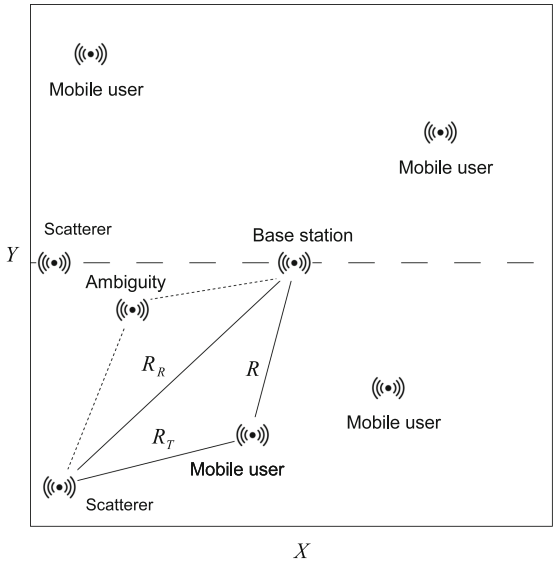

Fig. 1. Arrangement for mobile user localization and localization plane.

line of sight (LOS) to the base station. In the cell, several scatterers are also strategically positioned so that they have a clear LOS to both the base station and the mobile equipment.

Assume that the base station wants to localize a mobile unit of interest. A command is sent to that mobile equipment. The integrated radar system is activated and emits the radar signal. If the integrated radar system is a frequency-modulated continuous wave (FMCW), the passive receiver at the base station receives two delayed versions of the transmitted radar signal

$$S_1(\nu) = W\left(\nu - \kappa\frac{R}{\mathrm{c}}\right)\exp\left\{\frac{j2\pi\nu_{min}R}{\mathrm{c}} - j\pi\kappa\left(\frac{R}{\mathrm{c}}\right)^2\right\} \tag{1}$$

and

$$S_2(\nu) = W\left(\nu - \kappa\frac{R_T + R_R}{\mathrm{c}}\right)\exp\left\{\frac{j2\pi\nu_{min}(R_T + R_R)}{\mathrm{c}} - j\pi\kappa\left(\frac{R_T + R_R}{\mathrm{c}}\right)^2\right\} \tag{2}$$

where τ denotes range time and c is the speed of the wave propagation. If $w(\tau)$ is the envelope of the FMCW radar output, then $W(\nu)$ is the range compressed envelope in the ν domain. If $w(\tau)$ is a rectangular window, $W(\nu)$ will be a sinc function and if $w(\tau)$ is a tapered window, $W(\nu)$ will be a sinc-like function with lower sidelobe. The radar signal in the time-frequency analysis is a ramp signal with the start frequency ν_{min} and with the slope κ. The modulation time T results in a bandwidth of $B = \kappa T$. In (1) and (2), R, R_T and R_R denote the ranges (distances) between the base station and the mobile equipment of

interest, between the mobile user and the scatterer, and between the scatterer and the base station, respectively.

The localization plane (X, Y) is defined by the ground-range plane. The center of the plane is selected by the position of the base station as shown in Fig. 1. The delayed versions of the radar signal $S_1(\nu)$ and $S_2(\nu)$ are backprojected into the localization plane [16]. The backprojection process results in two visible circles (or one circle and one ellipse) in the localization plane. One circle corresponds to the monostatic radar measurement (mobile equipment - base station) and it is the intersection of the sphere of radius $\hat{R}$ with the localization plane

$$\begin{cases} \Im(X,Y) = S_1\left(\hat{R}\right) \exp\left\{ -\dfrac{j2\pi\nu_{min}\hat{R}}{\mathrm{c}} + j\pi\kappa\left(\dfrac{\hat{R}}{\mathrm{c}}\right)^2 \right\} \\ \hat{R} = \sqrt{X^2 + Y^2 + \Delta Z^2} \end{cases} \tag{3}$$

where ΔZ denotes the difference in height between the base station and the mobile equipment. The other corresponds to the bistatic radar measurement (mobile equipment - scatterer - base station) and it is the intersection of the sphere of radius $\hat{R}_T$ with the localization plane

$$\begin{cases} \Im(X,Y) = S_2\left(t, \hat{R}_T + R_R\right) \exp\left\{ -\dfrac{j2\pi\nu_{min}\left(\hat{R}_T + R_R\right)}{\mathrm{c}} + j\pi\kappa\left(\dfrac{\hat{R}_T + R_R}{\mathrm{c}}\right)^2 \right\} \\ \hat{R}_T = \sqrt{(X - X_S)^2 + (Y - Y_S)^2 + \Delta Z_S^2} \end{cases} \tag{4}$$

where ΔZ_S is the difference in height between the scatterer and the mobile user, and (X_S, Y_S) indicates the position of the scatterer. The intersection of the two circles in the localization plane localizes the mobile equipment of interest.

3 Multiple Mobile Equipment Localization

There are several technical issues with the localization approach presented in the previous section, in which the localization ambiguity needs to be solved. The ambiguity can be avoided if the scatter is strategically positioned, and the cell is divided into a number of sectors.

Figure 1 considers the case where a cell is divided into two sectors 0°–180° and 180°–360°, separated by the dashed line. There should be two directional antennas that are deployed and oriented to two sectors. The localization plane is also divided in to two parts 0°–180° and 180°–360°. Assume that, there is one mobile equipment that is object to be localized in the sector 180°–360°. According to the localization approach, the localization result is given by the intersection of two circles in the localization plane. This can give two localization results for the same mobile equipment of interest as the intersection of two circle can be two different points. One point corresponds to the true position of the mobile equipment, whereas the other is its image that is symmetrical to the true

position of the mobile equipment with respect to R_R. In Fig. 1, this point is marked by the text "Ambiguity" in the part 180°–360° of the localization plane. Cell sectoring is therefore only the necessary condition to avoid the localization ambiguity. The sufficient condition is that the scatterer must be strategically positioned.

Figure 1 suggests how to position a scatterer to avoid the localization ambiguity. In the case where the cell is divided into two sectors, the scatterer should be placed in the border of two sectors (the dashed line). There will be a single intersection of two circles lying in the part 180°–360° of the localization plane. The part 0°–180° of the localization plane is excluded from the backprojection process. The localization result is therefore unique.

Similarly, if the mobile equipment of interest is in the sector 0°–180°, the localization result will be given by a single intersection and in the part 0°–180° of the localization plane. The part 180°–360° of the localization plane is excluded from the backprojection process. The localization result is therefore unique.

With such, two mobile units can be localized a time slot and a frequency resource block.

The considered cell can also be divided into four sectors, 0°–90°, 90°–180°, 180°–270° and 270°–360°. In this case, there should be four directional antennas and they are deployed and oriented to four sectors. The localization plane is divided correspondingly into four parts. With strategical positioning scatters, four mobile units can be localized a time slot and a frequency resource block.

4 Simulation Results

In this section, we present some simulation results to examine and evaluate the proposal introduced in Sect. 3. The same scenario given in Fig. 1 is considered in the simulations.

4.1 System Parameters

Several mobile units operate in a microcell and served by a base station. Each mobile unit is equiped with a FMCW radar system. The parameters of the radar system are summarized in the first part Table 1. The radar system parameters are identical to the ones of 2πSENSE, a D-band FMCW radar [15]. The radar system can share the same antenna of the mobile equipment, giving omni-directional pattern.

The cell is divided into two sectors (0°–180°) and (180°–360°). Two passive receivers with two directional antennas are deployed at the base station. Each antenna is oriented to one sector. The simulation parameters for the base station are given in the second part of Table 1.

The scatterer is positioned at the border of two sectors. The radar cross section of the scatterer is normalized so that the signal attenuation is excluded. The simulation parameters for the scatterer are given in the third part of Table 1.

Table 1. Parameters FMCW radar system and scenario.

Parameter	Value
Mobile equipment	
Frequency span	126 GHz–182 GHz
Modulation time	$4.096 \cdot 10^{-3}$s
Duty cycle	$5 \cdot 10^{-3}$s
Antenna of mobile equipment	omni-directional
Mobile equipment antenna heights	1.8 m (0°–180°) 1.2 m (180°–360°)
Scatterer	
Characteristics	point-like scatterers
Scatterer height	5 m
Radar cross sections	$1\,\text{m}^2$
Scatterer - mobile eqipment range	12 m (0°–180°) 10 m (180° − 360°)
Base station	
Number of passive receivers	2
Antennas	directional
Base station antenna height	5 m
Base station - scatterer range	5 m
Base station - mobile equipment range	8 m (0°–180°) 10 m (180° − 360°)

Figures 2(a) and (b) provide the range-compressed radar signals, obtained with a Fourier transform of the outputs of the FMCW radar systems. In the plots, we convert the range time to the radar range by multiplying the time axis with the speed of propagation, i.e., with the speed of light in vacuum.

The range-compressed radar signal given in Fig. 2(a) corresponds to the radar measurement in the sector 0°–180° of the cell. Two peaks can be observed at the radar ranges about 8 m and 17 m. One peak is the LOS radar signal coming from the mobile equipment in the sector 0°–180° and the other is the multipath delayed version via the scatterer. The radar ranges are matched with the simulation parameters given in Table 1, found in base station - mobile equipment range, and the sum of scatterer - mobile equipment range and base station - scatterer range.

In Fig. 2(b), the given range-compressed radar signal corresponds to the radar measurement in the sector 180°–360° of the cell. We can also observe two peaks at the radar ranges about 10 m and 15 m. One peak is the LOS radar signal coming from the mobile equipment in the sector 180°–360° and the other is the multipath delayed version via the scatterer. The radar ranges are also matched with the simulation parameters given in Table 1.

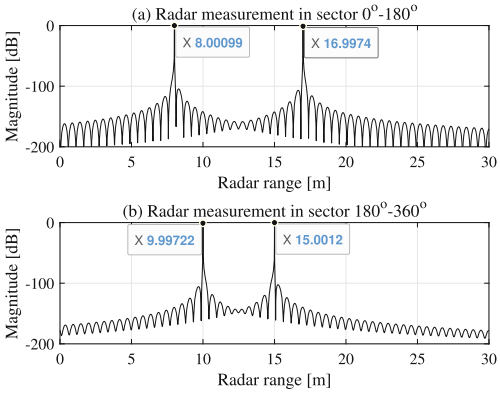

Fig. 2. Range-compressed radar signals.

4.2 Backprojection

As proved in [13], the accuracy of mobile user localization depends strongly on the assumptions on the differences in height between base station and mobile user ΔZ, and between scatterer and mobile user ΔZ_S. The heights of the base station and the scatterer are known, whereas the heights of mobile equipment are unknown and can vary in a wide range. They depend on the how tall the mobile users are and where the mobile equipment is placed, e.g., on a table and in the pocket of a mobile user. As suggested, in common cases, we can consider the range of $[1, 2]$ m for the height of mobile equipment. If we select the height of 1.5 for the backprojection process, the differences in height will be $\Delta Z = \Delta Z_S = 3.5$ m.

The backprojection of the range-compressed radar signal given in Fig. 2(a) into the part 0°–180° of the localization plane results in two halves of circle that can be observed in the upper part of Fig. 3. The intensity of the image pixels plotting the circles are identical to the peaks value of the range-compressed radar signal. The intersection of two halves of circle localizes a mobile unit at the coordinate $(5.50147, 4.63343)$ m. Compared with the parameters used in the simulations, the errors are estimated by $|\Delta X| = 0.0016$ m and $|\Delta Y| = 0.2154$ m.

The range-compressed radar signal given in Fig. 2(b) is backprojected into the part 180°–360° of the localization plane, resulting in four halves of circle. This effect is caused by the small separation between the peaks. Actually, two peaks of the range-compressed radar signal are close together. The backprojection processes consider both two peaks and each gives two circles. However, there is only an unique intersection of two halves of circle, localizing another mobile unit at the coordinate $(-2.25199, -9.04399)$ m. The errors are estimated by $|\Delta X| = 0.2479$ m and $|\Delta Y| = 0.1383$ m.

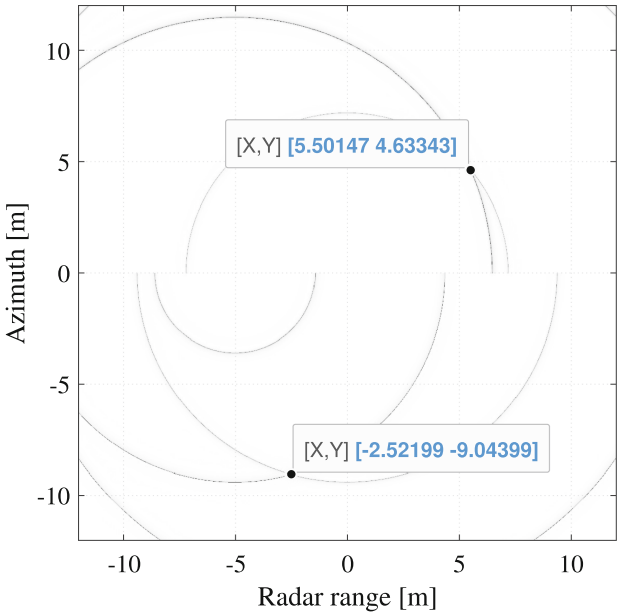

Fig. 3. Mobile user localization by implementing backprojection with unknown heights of mobile equipment. The value of 1.5 m is selected for the backprojection process.

4.3 Evaluation

To examine of the localization results, we can use the results to calculate the ranges based on (3) and (4). For the mobile equipment localized at the coordinate $(5.50147, 4.63343)$ m and with the height assumption of 1.5 m, (3) gives an estimation for the monostatic radar range (base station - mobile equipment range). A range of about 7.9991 m is retrieved. (4) gives an estimation for the bistatic radar range (mobile equipment - scatterer - base station range). A range of about $12 + 5 = 17$ m is retrieved. The estimations are almost identical to the parameters used in the simulation, verifying the localization results.

For the mobile equipment localized at the coordinate $(-2.25199, -9.04399)$ m and with the height assumption of 1.5 m, the estimated monostatic radar range is about 9.9557 m and the estimated bistatic radar range is about $10.0795 + 5 = 17.0795$ m. These vaues are also very close to the parameters used in the simulation.

The errors can be recognized in the localization results and can also be estimated. They are originated from the unknown heights of mobile equipment. In the simulations, we consider two mobile units with different heights (1.2 m and 1.8 m). An average height of 1.5 m is assumed and considered for all backprojection processes. This assumption leads to the different errors of the localization results. The maximum error is shown to be 0.25 m in the simulations and still

meets the demand of the localization at centimeter level in indoor environment for 6G [9].

Reaching a better level of accuracy for localization is also possible with three-dimension (3D) localization. In this case, the heights of mobile equipment will be estimated directly from the radar measurements. Armed with the information about the heights of mobile equipment, the localization results obtained with the 2D approach will be much more accurate. However, 3D localization requires more scatterers to be deployed and more radar measurements are also required. The computation complexity will therefore be increased.

4.4 Cell Sectoring and Multiple Mobile User Localization

In the simulations, a cell is divided into two sectors, helping to localize two mobile units at a time slot and a frequency resource block. As presented in Sect. 3, a cell can also be divided in to four sectors. Localizing fours mobile units at a time slot and a frequency resource block is therefore possible. A cell can be further divided into narrower sectors, e.g., 8 sectors, facilitating multiple mobile user localization but this might be unnecessary. There are the scheduling approaches in time and/or frequency that can be used for multiple mobile user localization.

As shown in [14], time scheduling is possible due to the small modulation time and small duty cycle of the radar system. For the duty cycle of 5 ms, 200 mobile units can be localized in one second. In combination with the cell sectoring with four sectors, the number of mobile units that can be localized is up to 800 in one second.

5 Practicality

The radar system parameters considered in the simulations are identical to the parameters of 2π SENSE, a D-band FMCW radar system [17]. The lower right of Fig. 4 shows the dimension of the FMCW radar in practice. The dimension of the electronic circuit is only about 2×3 cm, allowing an integration into mobile equipment. The electronic components of mobile equipment can also be used to build a FMCW radar system. Basically, integrating a radar system into mobile equipment is feasible.

5.1 FMCW Radar Operation

For a FMCW radar, the phase of the transmitted complex linear frequency-modulated chirp signal in the radio frequency (RF) domain can be expressed by [18]

$$\phi_{TX}(\tau) = \exp\left\{j2\pi\nu_{min}\tau + j\pi\kappa\tau^2\right\}, \quad 0 \leq \tau \leq T. \tag{5}$$

The chirp signal is assumed to propagate through a homogeneous medium. If there is a target at the range R, a part of the emitted chirp signal will be reflected

Fig. 4. Experiment setup for localization with indoor monostatic radar measurement using FMCW radar system.

to the radar system. The reflection is recorded by the receiver. The expression for the received signal due to the reflection is given by

$$\phi_{RX}(t,\tau) = \exp\left\{ j2\pi\nu_{min}\left(\tau - \frac{2R}{\mathrm{c}}\right) + j\pi\kappa\left(\tau - \frac{2R}{\mathrm{c}}\right)^2 \right\}. \tag{6}$$

The received signal is in the RF domain and needs to be downconverted to the intermediate frequency (IF) domain by mixing the transmitted and received signals. The result of the down-conversion is expressed by

$$\begin{aligned} \phi_{IF}(t,\tau) &= s_{TX}(\tau)\,\bar{s}_{RX}(t,\tau) \\ &= \exp\left\{ j2\pi\left(\nu_{min} + \kappa\tau\right)\frac{2R}{\mathrm{c}} - j\pi\kappa\left(\frac{2R}{\mathrm{c}}\right)^2 \right\}, \end{aligned} \tag{7}$$

where $\nu(\tau) = \nu_{min} + \kappa\tau$ denotes the linear modulated frequency of the chirp.

For range compression, the down-converted signal is transformed to the frequency domain using Fourier transform. The expression of the signal after Fourier transform is

$$S_{IF}(t,\nu) = W\left(\nu - \kappa\frac{2R}{\mathrm{c}}\right)\exp\left\{ \frac{j4\pi\nu_{min}R}{\mathrm{c}} - j\pi\kappa\left(\frac{2R}{\mathrm{c}}\right)^2 \right\} \tag{8}$$

The frequency shift defines a beat at

$$\nu_b = \kappa \frac{2R}{\mathrm{c}} \tag{9}$$

showing the relationship between the range R and the beat frequency ν_b. We can also rewrite (9) using the ramp duration T and the sweep bandwidth B as

$$\nu_b = \frac{B}{T}\frac{2R}{\mathrm{c}} \Leftrightarrow R = \frac{\mathrm{c}T}{2}\frac{\nu_b}{B} \tag{10}$$

Equation (8) is the standard equation for a FMCW radar system. Equations (1) and (2) have similar expressions but the range terms are different. In (1), since no reflection is considered, the factor 2 in (8) is excluded. In (2), the factor 2 in (8) is replaced by the sum of R_T and R_R.

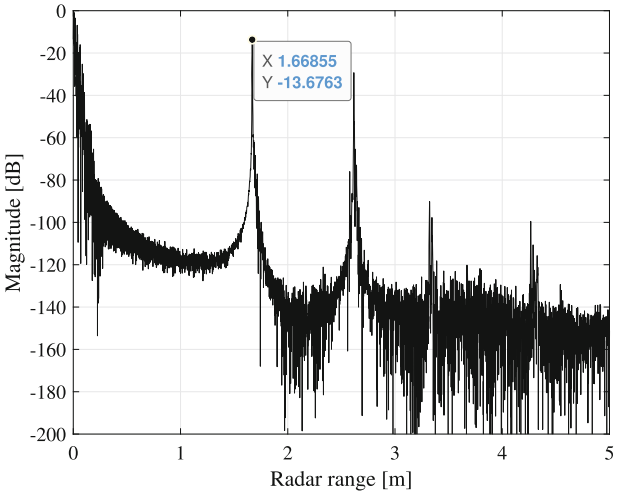

Fig. 5. Range-compressed radar signal provided by 2πSENSE.

5.2 Experiment

Figure 4 provides a simple measurement as a part of mobile user localization. The measurement is purely monostatic radar and carried out in the indoor environment. It is an office that is filled with furniture. The radar system is mounted at the height of about 2 m. A corner reflector is placed in front of the radar system with the range of about 1.6 m and at the height of about 1.5 m. Behind the corner reflector is the wall that is built with different materials including glass, wood and plastic. With this arrangement, the corner reflector plays the role of the mobile equipment with integrated radar system, whereas the radar system

plays the role of passive receiver with respect to the arrangement for mobile user localization. The radar system uses a horn, a directional antenna.

Figure 5 shows the range-compressed radar signal, obtained by a Fourier transform of 2πSENSEs output. A peak of the radar signal can be easily observed at the radar range $R \approx 1.7$ m, indicating the location of the corner reflector.

With the radar system parameters given in Table 1, we can calculate the radar signal bandwidth and then retrieve the range resolution. For the bandwidth of 56 GHz, the theoretical range resolution is down to 2.7 mm that is extremely accurate for localization.

6 Conclusion and Future Work

The paper discusses about the localization ambiguity and the approach for the problem. Cell sectoring is the necessary condition to avoid the localization ambiguity, whereas the sufficient condition is that the scatterer must be strategically positioned. The simulations examine and evaluate the multiple mobile equipment localization in indoor environment based on cell sectoring approach. A simple monostatic radar measurement partially shows the practicality of the approach.

The study will be continued with different extensions, resulting into different research topics. For example, hyper-accurate 3D localization in indoor environment for mobile equipment should be investigated in the future study. An investigation into non-stationary mobile equipment localization can also be a necessary study.

References

1. Kaushik, A., Vlachos, E., Thompson, J., Nekovee, M., Coutts, F.: Towards 6G: spectrally efficient joint radar and communication with radio frequency selection, interference and hardware impairment. IET Signal Process. **16**, 851–863 (2022)
2. de Oliveira, L.G., Nuss, B., Alabd, M.B., Diewald, A., Pauli, M., Zwick, T.: Joint radar-communication systems: modulation schemes and system design. IEEE Trans. Microwave Theory Tech. **70**(3), 1521–1551 (2022)
3. Bozorgi, F., Sen, P., Barreto, A.N., Fettweis, G.: RF front-end challenges for joint communication and radar sensing. In: IEEE JC&S, Dresden, Germany, pp. 1–6 (2021)
4. Sturm, C., Wiesbeck, W.: Waveform design and signal processing aspects for fusion of wireless communications and radar sensing. Proc. IEEE **99**(7), 1236–1259 (2011)
5. Herschfelt, A., Bliss, D.W.: Joint radar-communications waveform multiple access and synthetic aperture radar receiver. In: Proceedings of IEEE ACSSC, Pacific Grove, CA, USA, pp. 69–74 (2017)
6. Herschfelt, A., Bliss, D.W.: Spectrum management and advanced receiver techniques (SMART): joint radar-communications network performance. In: Proceedings of IEEE RadarConf, Oklahoma City, OK, USA, pp. 1078–1083 (2018)
7. Basit, A., et al.: Adaptive main lobe/sidelobes controls selection in FDA based joint radar-communication design. In: Proceedings of IEEE ICECCE, Swat, Pakistan, pp. (3) (2019)

8. Chen, X., Wei, Z., Fang, Z., Ma, H., Feng, Z., Wu, H.: Performance of joint radar-communication enabled cooperative UAV network. In: Proceedings of IEEE ICSIDP, Chongqing, China, pp. 1–5 (2019)
9. NGMN, 6G use cases and analysis. https://www.ngmn.org/wp-content/uploads/NGMN-6G-Use-Cases-and-Analysis.pdf
10. Sakhnini, A., Guenach, M., Bourdoux, A., Pollin, S.: A Cramr-Rao lower bound for analyzing the localization performance of a multistatic joint radar-communication system. In: IEEE JC&S, Dresden, Germany, pp. 1–5 (2021)
11. Ellison, S., Nanzer, J.A.: High-accuracy localization in joint radar and communications systems using multi-tone waveform modulation. In: IEEE AP-S/URSI, Montral, Qubec, Canada, pp. 1635–1636 (2020)
12. Kim, Y.H., Choi, J., Nemati, M.: Toward joint radar, communication, computation, localization, and sensing in IoT. IEEE Access **10**, 11772–11788 (2022)
13. Vu, V.T., Ivanenko, Y., Sjgren, T.K., Pettersson, M.I.: Realizing SAR for localization on mobile equipment with integrated radar system. In: Proceedings of IEEE IAICT, Bali, Indonesia, pp. 1–7 (2023, accepted for publication)
14. Vu, V.T., Ivanenko, Y., Batra, A., Sjgren, T.K., Pettersson, M.I., Kaiser, T.: Implementing backprojection at base station for precise localization in indoor environment. In: Proceedings of IEEE RIVF, Hanoi, Vietnam, pp. 1–6 (2023, submitted for publication)
15. Beard, C., Stallings, W.: Wireless Communication Networks and Systems, 1st edn. Pearson, London, UK (2015)
16. Hellsten, H., Andersson, L.E.: An inverse method for the processing of synthetic aperture radar data. Inverse Probl. **3**(1), 111–124 (1987)
17. Kueppers, S., Jaeschke, T., Pohl, N., Barowski, J.: Versatile 126–182 GHz UWB D-band FMCW radar for industrial and scientific applications. IEEE Sens. Lett. **6**(1), 1–4 (2021)
18. Skolnik, M.I.: Radar Handbook, 2nd edn. McGraw-Hill, New York (1990). ch. 16